Flying Particle Thermosensor in Hollow-Core Fiber Based on Fluorescence Lifetime Measurements

Jasper Freitag, Max Koeppel, Maria N. Romodina, Nicolas Y. Joly, and Bernhard Schmauss, *Member, IEEE*

***Abstract*—Thermosensitive fluorescence lifetime measurements enable accurate thermometry independent of intensity fluctuations along the optical path. Here, we report lifetime-based temperature measurements of a single europium-doped particle optically trapped in an air-filled hollow-core fiber. A frequency-domain fluorescence lifetime measurement setup was integrated into a dual-beam optical trap. The measured apparent lifetime shows a linear temperature dependence of -1.8 µs/K for excitation at 400 Hz. The results were repeatable over multiple cooling and heating cycles. In addition to temperature sensing, the influence of the high-power trapping laser on the measured apparent lifetime and fluorescence intensity was investigated. The observed laser-induced particle heating can be exploited to increase the fluorophore's sensitivity and operating range for low-temperature sensing. Fluorescence lifetime measurements of optically trapped particles inside a hollow-core fiber are promising for temperature sensing with micrometer spatial resolution over meter-scale distances.**

***Index Terms*—Frequency-domain fluorescence lifetime, hollow-core fiber, optical trapping, flying particle temperature sensor.**

I. Introduction

FIBER optic sensors that exploit temperature-dependent scattering or reflections along a sensing fiber are widely used for distributed temperature measurements in harsh environments [1], [2], [3], [4], [5]. As a new versatile optical sensor platform, flying particle sensors based on optically levitated microparticles inside a hollow-core fiber (HCF) have been introduced [6]. In principle, such sensors allow sensing of various physical quantities with micrometer-scale spatial resolution over kilometer-long distances. Distributed temperature sensing has been demonstrated by monitoring the speed of an optically propelled particle along a HCF using Doppler velocimetry or coherent optical frequency domain reflectometry [6], [7]. Although a spatial resolution in the µm-range seems feasible based on the reported localization precision of stationary trapped particles [8], such sensor resolutions have not yet been achieved with speed-based flying particle sensors. This results from the particle movement during the data acquisition and unavoidable temperature-independent speed variations along the HCF caused by fiber losses, coupling instabilities or intermodal beating [9]. Moreover, the sensitivity of these systems to thermally induced air flows, i.e., Knudsen pumps, is leading to erroneous results in fiber regions with strong temperature gradients [10]. Fluorescence-based flying particle sensors eliminate the need of continuous particle propulsion and are promising candidates to unlock the full potential of flying particle sensors in terms of spatial resolution [11], [12].

Thermosensitive fluorophores have been used for non-destructive, accurate temperature measurements with microscopic resolution based on a variety of different sensing mechanisms [13], [14]. For instance, the temperature-dependent change in fluorescence intensity can be exploited as a sensing mechanism. This method is simple to implement but sensitive to any change of losses occurring along the optical path [15]. Fluorescence-based methods that are independent of excitation and emission variations along the fiber are advantageous. Wavelength shifts of the peak fluorescence emission of an optically trapped fluorescent particle inside a HCF were used as an intensity-independent sensing quantity for temperature measurements [12]. However, this method requires a relatively long data acquisition to resolve fine wavelength shifts of a single emitting particle. Fluorescence lifetime is a more promising sensing quantity as methods based on this intrinsic fluorophore property are self-referencing, i.e., they require no calibration measurement and only a single-channel readout [14], [16]. Fluorescence lifetime imaging (FLIM) measurements allow high-spatial and temporal resolution measurements and are hardly affected by photobleaching or intensity changes along the optical path [13]. Although lifetime measurements have been previously combined with an optical trap for microfluidic

Manuscript received 2 August 2023; revised 2 October 2023; accepted 13 October 2023. Date of publication 17 October 2023; date of current version 15 December 2023. This work was supported by the Deutsche Forschungsgemeinschaft (DFG, German Research Foundation) under Grant 418737652. *(Corresponding author: Jasper Freitag.)*

This work did not involve human subjects or animals in its research.

Jasper Freitag is with the Institute of Microwaves and Photonics, Friedrich-Alexander-Universität, 91058 Erlangen, Germany (e-mail: jasper.freitag@fau.de).

Max Koeppel is with the Institute of Microwaves and Photonics, Friedrich-Alexander-Universität, 91058 Erlangen, Germany, and also with the Graduate School in Advanced Optical Technolgoies, 91052 Erlangen, Germany (e-mail: max.koeppel@fau.de).

Maria N. Romodina is with the Max Planck Institute for the Science of Light, 91058 Erlangen, Germany (e-mail: maria.romodina@mpl.mpg.de).

Nicolas Y. Joly is with the Department of Physics, Friedrich-Alexander-Universität, 91054 Erlangen, Germany, also with the Max Planck Institute for the Science of Light, 91058 Erlangen, Germany, and also with the Interdisciplinary Center for Nanostructured Films, 91058 Erlangen, Germany (e-mail: nicolas.joly@fau.de).

Bernhard Schmauss is with the Institute of Microwaves and Photonics, Friedrich-Alexander-Universität, 91058 Erlangen, Germany, also with the Graduate School in Advanced Optical Technologies, 91052 Erlangen, Germany, and also with the Max Planck Institute for the Science of Light, 91058 Erlangen, Germany (e-mail: Bernhard.Schmauss@fau.de).

Color versions of one or more figures in this article are available at https://doi.org/10.1109/JSTQE.2023.3325374.

Digital Object Identifier 10.1109/JSTQE.2023.3325374

temperature measurements [17] no lifetime-based sensor using optically trapped particles inside a HCF has been realized yet. Therefore, it has not been possible to combine the microscopic resolution and high accuracy of lifetime-based sensors with the long measurement range of fiber optic sensors. In addition, no lifetime-based temperature measurements of optically levitated particles in air were reported yet. Such measurements can be used to study heat dissipation and non-equilibrium thermodynamics at low pressures in levitated optomechanical systems and novel ultrasensitive sensing schemes [18], [19].

In this work, we demonstrate temperature sensing based on fluorescence lifetime measurements of a europium-doped particle, which is optically trapped inside a HCF. For this, a frequency-domain fluorescence lifetime measurement system was integrated into a particle trapping setup.

II. Materials and Methods

A. Europium-Doped Particles as Lifetime-Based Thermosensors

Fluorescence lifetime measurements have been employed for temperature sensing using particles with europium complexes incorporated into the polymer. These fluorescent particles provide a narrow emission band at $\sim 613\,\mathrm{nm}$, a large Stokes shift, and an intensity decay time in the range of hundreds of microseconds [13], [20], [21]. These favorable properties result from the energy transfer from an organic ligand of the europium chelate, which absorbs UV light, to the europium ion through the triplet state of the ligand [22]. Experiments with europium-based fluorophores have been demonstrated to show lifetime-temperature sensitivities up to -10 µs/K for temperature ranges between 280 K and 360 K [20], [21], [23], [24], [25]. In this work, we used europium-doped polystyrene particles with a diameter of 4 µm and a doping concentration below 0.2% that were fabricated by Microparticles GmbH, Berlin.

B. Frequency Domain Fluorescence Lifetime Measurement

FLIM techniques are typically categorized into time-domain and frequency-domain measurement techniques [26]. In this study, the frequency-domain method is used as it provides highly accurate results for single-spot measurements [14]. In addition, this method does not require a costly pulsed laser [27]. Frequency-domain lifetime measurements are typically performed by exciting a fluorescent sample using a sinusoidally modulated light source. The emitted fluorescent light is phase shifted and less deeply modulated with respect to the excitation due to the fluorescence lifetime of the sample. By measuring this phase shift or change in modulation depth, information about the lifetime of the sample can be retrieved. In this work, an in-phase/quadrature technique was digitally implemented to determine the amplitude and phase of the modulated excitation (ex) and emission (em) signal. Based on the in-phase I and quadrature Q components of the signals their amplitudes A and phases ϕ are estimated for the modulation frequency as:

$$A = \sqrt{I^2 + Q^2} \tag{1}$$

$$\phi = \arctan\left(\frac{Q}{I}\right). \tag{2}$$

The phase shift between both signals is then calculated as

$$\Delta\phi = \phi_{\mathrm{em}} - \phi_{\mathrm{ex}} \tag{3}$$

and the relative modulation as [27]

$$M = \frac{A_{\mathrm{em}}}{A_{\mathrm{em,dc}}} \Big/ \frac{A_{\mathrm{ex}}}{A_{\mathrm{ex,dc}}} \tag{4}$$

where the index dc indicates the signal's average amplitude. The normalization using the dc components compensates for slightly varying fluorescence intensity between measurements due to particle movements caused by trapping laser power fluctuations and slightly varying coupling efficiencies of the trapping beams into the HCF. In addition, this normalization strategy is beneficial in the presented experiment due to the presence of thermal quenching and photobleaching even though dc components are typically more affected by noise and offsets [28].

Both quantities, $\Delta\phi$ and M, are independently related to the fluorescence lifetime, i.e., the fluorescence intensity decay as a function of time [29]. For a single exponential decay, the lifetimes calculated from the measured phase shift and relative modulation are equal, independent of the modulation frequency, and can be directly interpreted as molecular features of the fluorophore. For multi-exponential decay systems, both measurement methods result in different apparent lifetime values that depend on the modulation frequency [29]. Nevertheless, both quantities can be used as a sensitive measure for temperature that only requires fluorescence excitation at a single modulation frequency.

For each measurement, the apparent phase and modulation lifetime can be obtained from the phase shift and relative modulation [29]:

$$\tau_{\mathrm{app},\phi} = \frac{\tan(\Delta\phi)}{2\pi f_{\mathrm{mod}}} \tag{5}$$

$$\tau_{\mathrm{app},M} = \frac{1}{2\pi f_{\mathrm{mod}}}\sqrt{\frac{1}{M^2} - 1} \tag{6}$$

where f_{mod} is the modulation frequency. In this work, both values are averaged to a single apparent lifetime value

$$\tau_{\mathrm{app}} = \frac{\tau_{\mathrm{app},\phi} + \tau_{\mathrm{app},M}}{2} \tag{7}$$

that is used as a sensing quantity.

The maximum sensitivity of frequency-domain fluorescence lifetime measurements is achieved if the average expected lifetime is approximately equal to the inverse of the angular modulation frequency [27]. For this reason, a modulation frequency of $400\,\mathrm{Hz}$ or $600\,\mathrm{Hz}$ was used throughout the experiments corresponding to the above-mentioned fluorescence lifetime of europium-doped particles.

C. Combined Optical Trapping and Lifetime Measurement Setup

Fig. 1 depicts the combined particle trapping and fluorescence lifetime measurement setup.

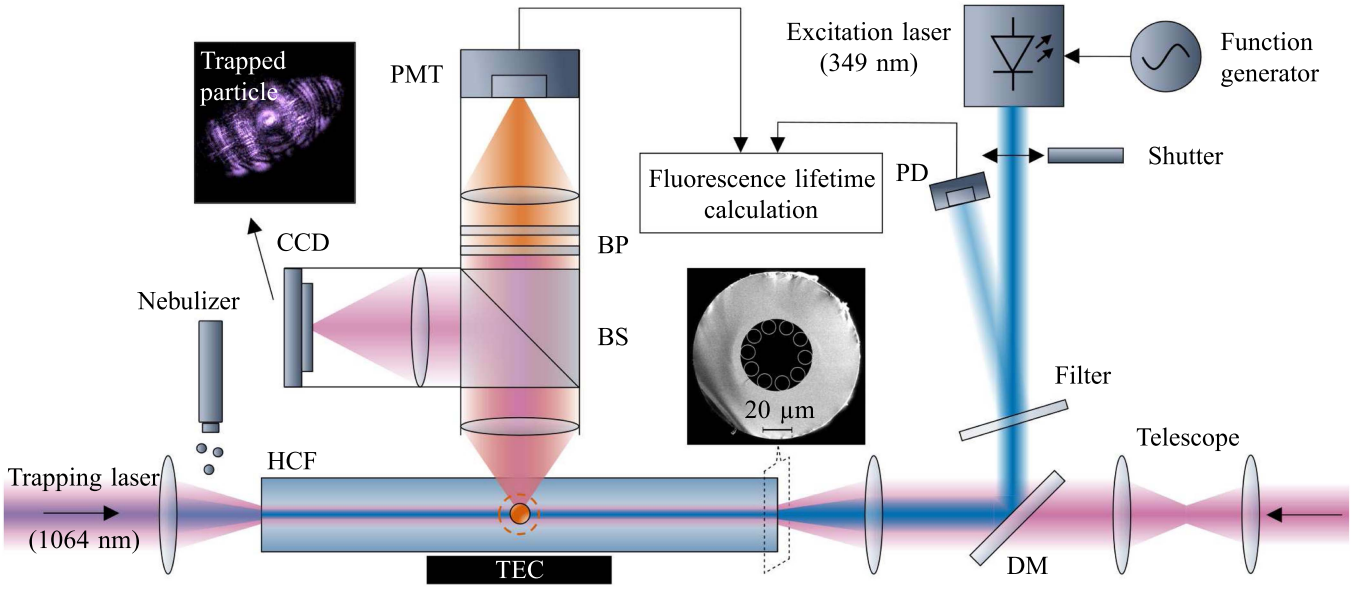

Fig. 1. Combined particle trapping and lifetime measurement setup: The nebulizer is used to spread europium-doped particles in front of the fiber end, where one of them is trapped and propelled into the hollow-core fiber (HCF) using two counter-propagating trapping laser beams (purple). The particle is excited from a UV laser (blue) that is sinusoidally modulated by a function generator and combined with the trapping laser using a dichroic mirror (DM). The fluorescence light emitted by the particle is collected by a high-NA lens, filtered using a narrow bandpass (BP), and detected using a photomultiplier tube (PMT). The detector was aligned by imaging a small fraction of the scattered light from the particle on a camera (CCD) reflected from a beamsplitter (BS). The apparent fluorescence lifetime for different thermoelectric cooler (TEC) temperatures is obtained from the detected fluorescence and excitation signal, measured by a photodiode (PD).

1) Trapping Setup: The trapping setup was realized by two counter-propagating laser beams coupled into a single-ring HCF with a core diameter of ~ 30 µm and a length of ~ 50 cm. Both trapping beams originate from the same linearly polarized laser source (1064 nm) and were split using a polarizing beamsplitter (PBS). The power ratio of both beams was adjusted using a half-wave plate (HWP) mounted on a motorized stage. An additional HWP and PBS were placed near the laser output to monitor the trapping power.

An uncoated fiber section of 3 cm, surrounded by air, was installed directly on top of a 3-cm-long metal block that was heated or cooled with a thermoelectric cooler (TEC). The temperature controller, operated with a PT100 temperature sensor (inserted into the metal block using thermally conductive paste), provides a temperature accuracy of ± 0.3 K. This TEC temperature read-out was recorded for every lifetime measurement.

2) Fluorescence Excitation: The fluorescent particle was excited by coupling the excitation laser into the HCF. This ensures illumination of the particle along the entire fiber and minimized background fluorescence compared to irradiation configurations from the fiber side. The intensity-modulated CW laser (Roithner Lasertechnik RLTUVL-349-10-10) emits at ~ 349 nm, which is close to the absorption peak of the europium-doped particles. The UV beam was combined into the beam path of the trapping laser using a dichroic mirror (DM) and coupled into the HCF using an uncoated lens. To compensate for the different focal lengths and optimize the beam diameters of the IR and UV laser a telescope was implemented. A coupling efficiency of more than 50% was achieved for both lasers.

The modulation of the excitation laser was recorded as a reference by tracking the reflection from a slightly tilted neutral density filter using a photodiode (PD). To prevent photodamaging of the europium-doped particle, the UV power coupled into the HCF was reduced to ~ 10 µW using this filter. Additionally, an antireflection-coated bandpass (BP) was installed behind the excitation laser to block additional spectral components. To probe the fluorescence response, the laser was sinusoidally modulated above the laser threshold with a modulation depth of ~ 0.6.

The particles suffer from photobleaching over time when they are exposed to UV irradiation. To minimize the irradiation duration, a motorized beam shutter was installed in front of the UV laser output.

3) Fluorescence Detection: When the particle is trapped by the IR laser and excited by the UV laser, light gets scattered and fluorescence light is emitted. This light was captured from the fiber side (see Fig. 1) using a microscope lens system mounted on a movable stage. This effectively limits the fluorescence detection to a single particle in the microscope's field of view. To gather a high fraction of this light and to minimize autofluorescence, occurring along the detection path, a high numerical aperture (NA)-lens (NA $= 0.54$) and a longpass filter (cut-off wavelength 500 nm) were used. Most of the light was used to observe the fluorescence with a photomultiplier tube (PMT) while a small fraction was reflected at a beamsplitter (BS) to monitor the particle's position by imaging the scattered IR light on a camera (CCD) (see inset Fig. 1). The scattered IR light was blocked by a shortpass filter (cut-off wavelength 750 nm) and a fluorescence filter (Edmund optics 87-753) with a center wavelength at 615 nm and a 20 nm passband. This limited the detectable wavelengths accordingly to the maximum emission band of the europium-doped particles. To validate the filter

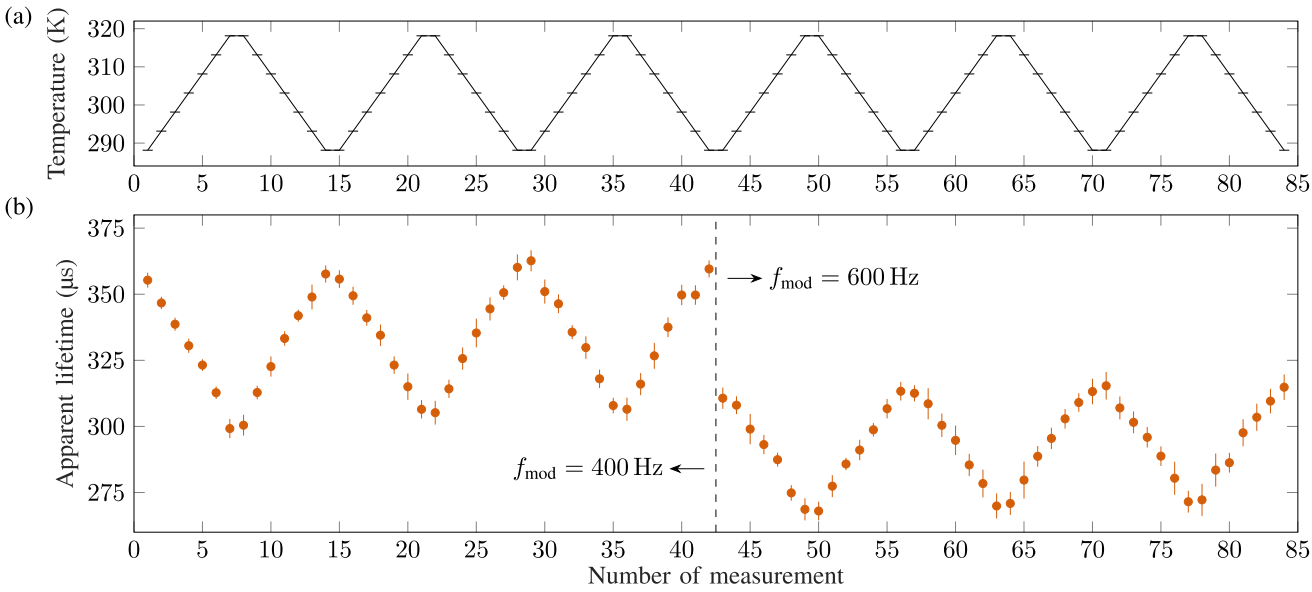

Fig. 2. Fluorescence lifetime-based temperature sensing. TEC temperature (a) and apparent lifetimes (b) measured for the same europium-doped particle, optically levitated inside the fiber using an optical trapping power of ~ 3.5 W. The excitation laser was modulated at 400 Hz for the first three heating and cooling cycles, and at 600 Hz for the following cycles. The error bars indicate the standard deviation of 8 measurements.

design, a non-fluorescent particle with a diameter of 3 µm was trapped and moved below the detector. The recorded signal of this particle was more than two orders of magnitudes lower than the signal of the fluorescent particle during UV illumination. Both the reference signal as well as the fluorescence signal were sampled at 500 kS/s with 14bit and stored for subsequent lifetime calculation.

D. Experimental Procedure

1) Lifetime-Based Temperature Sensing: A europium-doped particle was loaded into the optical trap from a particle droplet stream that was created by a nebulizer with a mesh size sufficiently small to prevent particle clustering. The nebulizer was directed towards the fiber end face via an inlet tube. A trapped particle was propelled inside the HCF and placed below the detector by manually adjusting the power ratio of the counter-propagating trapping beams. There, the particle was held stationary by making use of a stable trapping position formed by the intermodal beating between the fundamental and higher-order core modes. The detector's position was fine-tuned by imaging the IR light scattered from the particle on the CCD. After the ambient light was switched off the temperature sensing experiment was performed: For each temperature, the metal block was heated or cooled by the TEC to a target temperature. After the measured TEC temperature deviated by less than 0.02 K from the target temperature, the setup was allowed to settle for 15 s prior to starting the measurement. Then, the fluorescence and reference signal were recorded while the UV shutter was opened for 440 ms. This data was split into 8 segments of 55 ms, for which the apparent lifetimes were determined individually. To compensate for dc offsets present in both channels, both signals were additionally recorded for 20 ms before and after the UV shutter was closed.

2) Particle Heating Induced by the Trapping Laser: To investigate the influence of the trapping power on the measured lifetime a series of measurements was conducted, for which the total amount of trapping power was changed at a constant TEC temperature. Except for this, the experimental procedure remained unchanged.

III. Apparent Lifetime Measurement

A. Temperature Sensing

Fig. 2 shows the temperature dependence of the measured apparent lifetime for a single europium-doped particle trapped in a HCF. The TEC temperature was successively increased or decreased in steps of 5 K between 288.1 K and 318.1 K while the trapping power was set to ~ 3.5 W. Six heating and cooling cycles were recorded over a duration of ~ 52 min. During this time the particle was exposed to ~ 37 s of UV illumination. The modulation frequency was set to 400 Hz for the first three cycles and to 600 Hz for the following cycles. The measured data shows that an increase in the TEC temperature corresponds to a decrease in the apparent lifetime. This trend was repeatable for all heating or cooling cycles independent of the modulation frequency. The measured apparent lifetimes were in the range from 299 µs to 363 µs and 268 µs to 315 µs for a modulation frequency of 400 Hz and 600 Hz, respectively. The significantly lower apparent lifetimes measured for a higher modulation frequency suggest that the detected fluorescence signal is composed of multiple exponential decays [29]. This is further discussed in the Appendix.

The measured apparent lifetime as a function of the TEC temperature is presented in Fig. 3 for the first three heating and cooling cycles. The obtained lifetime values decrease approximately linearly as the temperature increases. By fitting the

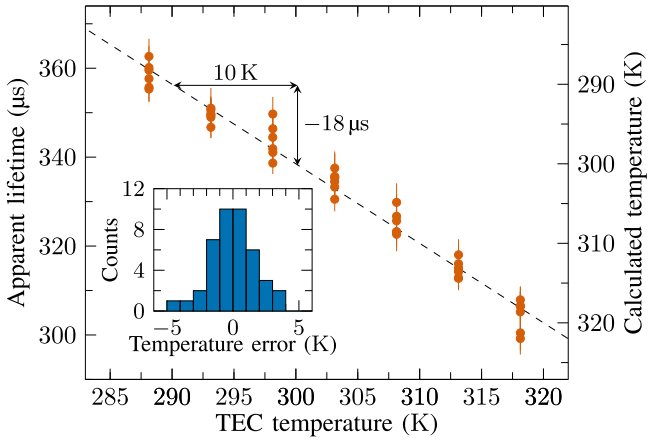

Fig. 3. Measured apparent lifetimes with error bars showing the standard deviation of 8 measurements as a function of the TEC temperature for three heating and cooling cycles using a modulation frequency of 400 Hz. The sensitivity was estimated to −1.8 µs/K based on the linear fit (dashed line). The calculated temperatures were retrieved from the measured apparent lifetimes using the linear fit. Inset: histogram of the temperature error.

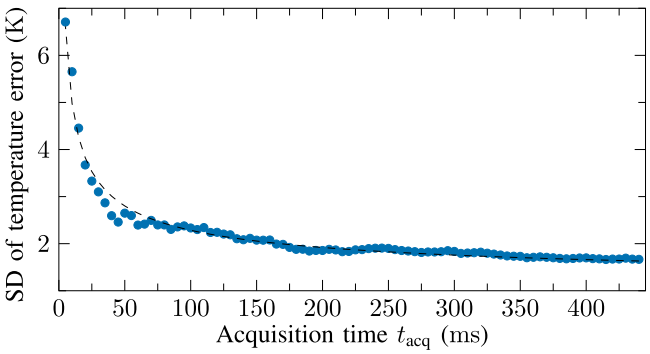

Fig. 4. Standard deviation (SD) of the temperature error as a function of the acquisition time for the measurements using a 400 Hz modulation. The length of time, used for the apparent lifetime calculation, was stepwise increased from 5 ms to the total acquired time of 440 ms. The dashed line represents the fit to $A_1/\sqrt{t_{acq}} + A_2$ with $A_1 = 12.48$ K$\sqrt{\text{ms}}$ and $A_2 = 1.04$ K.

results to a linear function, a sensitivity of −1.8 µs/K was estimated with a coefficient of determination $R^2 > 0.97$. A similar result was obtained for the heating and cooling cycles using a higher modulation frequency of 600 Hz. Here, a sensitivity of −1.4 µs/K was determined based on the measured apparent lifetimes with $R^2 > 0.97$.

Fig. 3 also shows the calculated temperatures derived from the measured apparent lifetimes using the plotted linear fit. The sensor's performance was evaluated by comparing the TEC temperatures with the calculated temperatures. The histogram of the temperature error is shown in the inset of Fig. 3 for the measurement series using a 400 Hz modulation. The resulting temperature errors are approximately Gaussian distributed with a standard deviation (SD) of 1.67 K. A maximum absolute error of 4.35 K was calculated. Similar results were obtained for the measurement with a modulation frequency of 600 Hz. Here, a maximum absolute temperature error of 3.15 K and a SD of 1.45 K were determined.

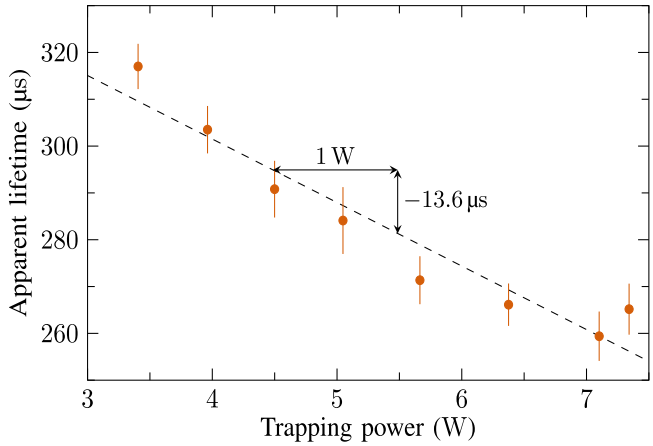

Fig. 5. Measured apparent lifetime and linear fit (dashed line) of a fluorescent particle using different trapping powers at a TEC temperature of 288.1 K. The error bars are determined by the standard deviation of 8 measurements.

In Fig. 4, the sensor's precision is analyzed with respect to the acquisition time t_{acq}. The SD of the temperature error was evaluated for a length of time ranging from 5 ms to 440 ms. The fit to the function $A_1/\sqrt{t_{acq}} + A_2$ (see Fig. 4) reveals that the error is approximately inversely proportional to the square root of the acquisition time. This is consistent with the Cramer-Rao lower bound for single-frequency phase and amplitude estimation from noisy discrete-time data with known frequency [30]. The fitting parameter $A_2 = 1.04$ K indicates the minimum temperature error achievable with this setup for infinitely long measurements while neglecting additional photobleaching or system drifts. To achieve a SD of 2.5 K, a data acquisition time of 73 ms would be sufficient based on the fit.

B. *Trapping Power Dependence*

Fig. 5 shows the influence of the trapping power on the measured lifetime. An increase in the trapping power from 3.4 W to 7.3 W leads to a decrease in the measured apparent lifetime with a slope of −13.6 µs/W (coefficient of determination $R^2 > 0.92$). The same trend was observed for higher TEC temperatures. This indicates that the europium-doped particle is heated by the absorption of IR light from the trapping laser.

To further analyze this effect, we determined the temperature-dependent apparent lifetime of the europium-doped particle in absence of IR illumination. The apparent lifetimes were measured during a cooling cycle with temperature decrements of 5 K, followed by a subsequent heating cycle with temperature steps of 10 K. This measurement was performed with a single particle that was trapped in front of the fiber and propelled into the HCF, until it reached the heatable fiber section. After aligning the detector the trapping laser was switched off to drop the particle onto the inner fiber wall. Although the particle was stuck on the fiber wall it was still possible to excite the particle using the UV laser through the fiber core. The resulting lifetime-temperature curve, presented in Fig. 6, shows an overall increase in the apparent lifetime compared to the particle that was optically trapped by the high-power IR laser. The measured values ranged

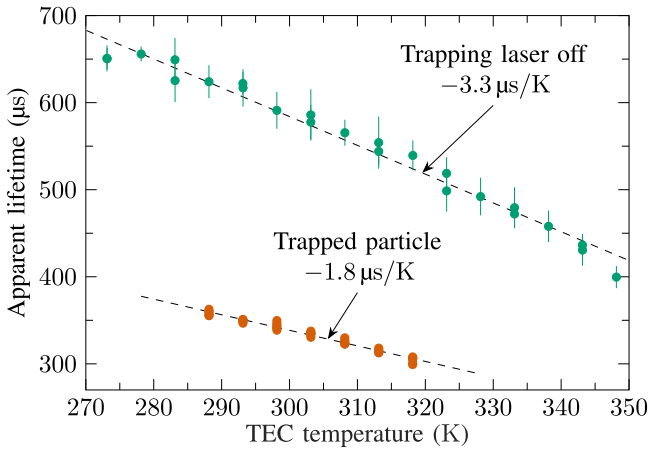

Fig. 6. Measured apparent lifetimes for different TEC temperatures of a particle collapsed to the inner fiber wall after switching off the trapping laser in comparison to a trapped particle (data set from Fig. 3) using a 400 Hz modulation. The error bars indicate the standard deviation of 8 measurements.

from 656 µs to 400 µs for temperatures between 273.1 K and 348.1 K and revealed a steeper slope of −3.3 µs/K (coefficient of determination $R^2 > 0.97$). The exemplary evaluation of the fitted results at room temperature (RT) shows an increase in apparent lifetime of ∼255 µs due to laser-induced particle heating. Apparent lifetimes measured in absence of the trapping laser for an extended temperature range were significantly higher than for a trapped particle at low temperature. This indicates that the particle was heated to more than ∼55 K above RT when exposed to the ∼3.5 W trapping laser. The upper limit of the laser-induced particle heating was estimated to ∼95 K above RT by extrapolating the apparent lifetime curve for higher temperatures using the denoted slope of the trapped particle.

IV. Discussion

The apparent lifetime measurements of optically trapped particles revealed robust and repeatable results despite the strong fluctuations and photobleaching present in the detected signal as discussed in the Appendix. This confirms the advantageous use of lifetime-based sensor concepts for distributed flying particle sensors with unavoidable intensity variations along the fiber. The presented frequency-domain lifetime measurements allows dynamic temperature sensing, for which the measurement rate can be adapted to the desired temperature precision (see Fig. 4).

The amplitude of the fluorescence signal decreases as the particle temperature increases due to the thermal quenching of the fluorophore (see Appendix). Therefore, the significant laser-induced particle heating lowers the signal-to-noise ratio of the detected PMT signal. Moreover, the sensor's sensitivity was reduced by the laser-induced particle heating as evident from the data presented in Fig. 6. This finding is consistent with prior lifetime measurements of europium compounds, in which the observed temperature-dependent fluorescence response is less sensitive at higher temperature regimes [20], [23]. For such a wide range of temperatures, the lifetime-temperature curve of europium-doped particles cannot be linearized accurately and should instead be described by an Arrhenius-type equation [20], [24]. Fluctuations of the IR power distort the lifetime-based temperature measurements as a result of the laser-induced particle heating. This influence can be mitigated by tracking the IR power and subsequent compensation. Despite these disadvantages, this heating mechanism can also be beneficial to shift the operating point of this sensor along the nonlinear lifetime-temperature curve to achieve maximum sensitivity. This is in particular interesting for sensing low temperatures, which may be completely outside the usual operating temperature range of the fluorescent probe.

In addition to its use as a thermosensor, the optical trap inside the HCF can also be used as a scientific chamber to analyze the particle itself or its local environment. This setup introduces a novel method for studying microfluidic channels using fluorescent probes, eliminating the need for cleaning procedures and minimizing potential effects associated with surface contact or light contamination [31], [32], [33]. For this purpose, the presented technique can be extended to track multi-exponential decay components using multiple modulation frequencies (see Appendix).

V. Conclusion

This work investigated the potential of fluorescence-lifetime thermometry using fluorescent microparticles optically trapped inside a HCF. The presented apparent lifetime measurements of a single europium-doped particle revealed a sensitive, linear, and repeatable temperature dependence that can be directly applied for lifetime-based temperature sensing. The sensor's robustness was demonstrated by achieving a temperature error below 1.7 K despite the presence of intensity fluctuations caused by particle movements during six heating and cooling cycles of 30 K. This combined particle trapping and fluorescence lifetime measurement setup paves the way for distributed temperature sensing using flying fluorescent particles. While the fluorescence emission of a stationary particle was detected from the fiber side in this study, the setup can be modified to capture the fluorescence response of an optically propelled particle from the fiber end face. This modification allows the demonstration of remote temperature sensing with moving particles using the HCF's broad transmission spectrum. Moreover, integrating a particle localization system [7] into the setup holds the potential for sensing applications with micrometer-scale resolution over long measurement ranges.

Appendix
Robustness of the Lifetime Measurement

The robustness of this lifetime-based sensor against signal fluctuations can be seen in Fig. 7. The determined apparent lifetimes were highly repeatable for the heating and cooling cycles (see Fig. 7(a)) despite the strong power variations in the detected signal, as evident in Fig. 7(b). The observed overall intensity decrease is caused by photobleaching and relates to the accumulated UV power to which the europium-doped particle was exposed. Furthermore, we noticed that increasing the trapping laser power accelerates the photobleaching process.

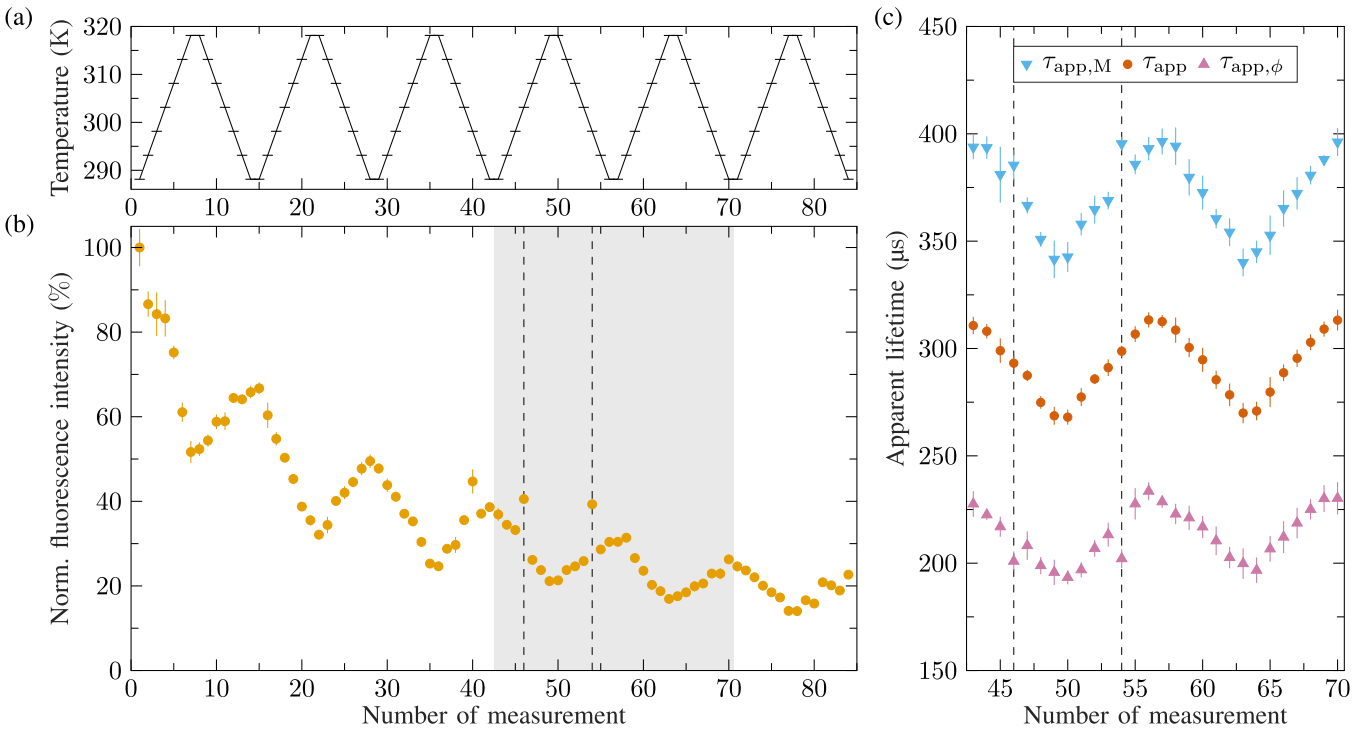

Fig. 7. Measurements of fluorescence intensity and apparent lifetime for the presented temperature sensing experiment. (a) TEC temperature. (b) Mean fluorescence intensity of each measurement, normalized to the initial intensity. The recorded intensity decreases as temperature increases and over the number of measurements due to photobleaching caused by the UV laser. Outliers, exemplarily indicated by dashed lines, are most likely the result of particle movements that were caused by trap instabilities and observed from the scattered IR light on a CCD. (c) Apparent lifetimes calculated as the arithmetic mean of the apparent phase- and modulation-based lifetime for the measurements highlighted by the gray area. The error bars are obtained from the standard deviation of 8 measurements.

The overall photobleaching can be reduced by using a higher modulation depth, a lower trapping power, a trapping laser wavelength that is less absorbed by the europium-doped particle, or by optimizing the chemical composition of the used europium complexes and host material [22], [34]. However, a full investigation of the photobleaching and laser-induced heating process is beyond the scope of this work. Intensity changes also result from fluorescence quenching processes that are induced by temperature variations. In Fig. 7(b) a few intensities peaks, exemplarily indicated by the dashed lines, were present. We believe that these peaks are caused by slight particle movements of approximately 20 µm that we observed during the trapping experiment on the CCD. These movements vary the amount of light captured by the detector setup.

By comparing the measurements, for which intensity peaks were apparent, it was noticeable that changes in phase- and modulation-based apparent lifetimes compensated for each other. This effect may be attributed to the influence of changes of zero, short, or long lifetime components, i.e., UV scattering, background fluorescence, or phosphorescence, in the detected signal and is subject to further investigation.

The calculation of the apparent lifetime as the arithmetic mean of the phase and modulation apparent lifetime is shown in Fig. 7(c). The individual measurement of the modulation-based apparent lifetime was throughout all experiments higher than the phase-based value. This indicates multi-exponential decay components in the detected signal [29] and results from the highly nonlinear phase- and modulation measurement technique [35]. The presence of multiple lifetime components is consistent with the overall smaller lifetimes that were measured for the higher modulation frequency [29]. In addition, this finding is supported by a previous study with europium complexes, in which multi-exponential decay curves were observed for higher temperatures [22].

Due to the observed laser-induced particle heating it must be assumed that multi-exponential decay characteristics were present during the trapping experiments. Therefore, the measured apparent lifetimes cannot be directly interpreted as molecular features of the fluorescent probe. However, the apparent lifetime measurement of the optically trapped europium-doped particle has been shown to provide a repeatable and sensitive measure applicable for thermometry. Moreover, the accuracy of this frequency-domain lifetime measurement technique can be improved by using multiple modulation frequencies to monitor multiple lifetime components, present in the detected signal, and to suppress unavoidable background fluorescence [36], [37].

ACKNOWLEDGMENT

The authors would like to thank Prof. Shangran Xie for fruitful discussions and suggestions.

REFERENCES

[1] A. Ukil, H. Braendle, and P. Krippner, "Distributed temperature sensing: Review of technology and applications," *IEEE Sensors J.*, vol. 12, no. 5, pp. 885–892, May 2012.

[2] B. Lee, "Review of the present status of optical fiber sensors," *Opt. Fiber Technol.*, vol. 9, no. 2, pp. 57–79, 2003.

[3] D. K. Gifford et al., "Swept-wavelength interferometric interrogation of fiber Rayleigh scatter for distributed sensing applications," *Fiber Optic Sensors Appl. V*, vol. 6770, 2007, Art. no. 67700F.

[4] B. Lee, S. Roh, and J. Park, "Current status of micro- and nano-structured optical fiber sensors," *Opt. Fiber Technol.*, vol. 15, no. 3, pp. 209–221, 2009.

[5] M. De, T. K. Gangopadhyay, and V. K. Singh, "Prospects of photonic crystal fiber as physical sensor: An overview," *Sensors*, vol. 19, no. 3, 2019, Art. no. 464.

[6] D. S. Bykov, O. A. Schmidt, T. G. Euser, and P. St. J. Russell, "Flying particle sensors in hollow-core photonic crystal fibre," *Nature Photon.*, vol. 9, no. 7, pp. 461–465, 2015.

[7] M. Koeppel et al., "Doppler optical frequency domain reflectometry for remote fiber sensing," *Opt. Exp.*, vol. 29, no. 10, 2021, Art. no. 14615.

[8] J. Podschus et al., "Position measurement of multiple microparticles in hollow- core photonic crystal fiber by coherent optical frequency domain reflectometry," in *Proc. Opt. Fiber Sensors Conf.*, 2020, pp. W1–2.

[9] M. K. Garbos, T. G. Euser, O. A. Schmidt, S. Unterkofler, and P. St.J. Russell, "Doppler velocimetry on microparticles trapped and propelled by laser light in liquid-filled photonic crystal fiber," *Opt. Lett.*, vol. 36, no. 11, pp. 2020–2022, 2011.

[10] O. A. Schmidt, M. K. Garbos, T. G. Euser, and P. St. J. Russell, "Reconfigurable optothermal microparticle trap in air-filled hollow-core photonic crystal fiber," *Phys. Rev. Lett.*, vol. 109, no. 2, 2012, Art. no. 024502.

[11] R. Zeltner et al., "Fluorescence-based remote irradiation sensor in liquid-filled hollow-core photonic crystal fiber," *Appl. Phys. Lett.*, vol. 108, no. 23, 2016, Art. no. 231107.

[12] R. Zeltner, R. Pennetta, S. Xie, and P. St. J. Russell, "Flying particle microlaser and temperature sensor in hollow-core photonic crystal fiber," *Opt. Lett.*, vol. 43, no. 7, 2018, Art. no. 1479.

[13] M. M. Ogle, A. D. S. McWilliams, B. Jiang, and A. A. Martí, "Latest trends in temperature sensing by molecular probes," *ChemPhotoChem*, vol. 4, no. 4, pp. 255–270, 2020.

[14] X. Wang, O. S. Wolfbeis, and R. J. Meier, "Luminescent probes and sensors for temperature," *Chem. Soc. Rev.*, vol. 42, no. 19, 2013, Art. no. 7834.

[15] H. Szmacinski and J. R. Lakowicz, "Measurement of the intensity of long-lifetime luminophores in the presence of background signals using phase-modulation fluorometry," *Appl. Spectrosc.*, vol. 53, no. 12, pp. 1490–1495, 1999.

[16] A. P. Demchenko, "Fluorescence detection in sensor technologies," in *Introduction Fluorescence Sens.*, vol. 395, 3rd ed., New York, NY, USA: Springer, 2020 pp. 55–110.

[17] M. A. Bennet et al., "Optically trapped microsensors for microfluidic temperature measurement by fluorescence lifetime imaging microscopy," *Lab Chip*, vol. 11, no. 22, 2011, Art. no. 3821.

[18] A. T. M. A. Rahman and P. F. Barker, "Laser refrigeration, alignment and rotation of levitated Yb^{3+}: YLF nanocrystals," *Nature Photon.*, vol. 11, no. 10, pp. 634–638, 2017.

[19] G. P. Conangla, A. W. Schell, R. A. Rica, and R. Quidant, "Motion control and optical interrogation of a levitating single nitrogen vacancy in vacuum," *Nano Lett.*, vol. 18, no. 6, pp. 3956–3961, 2018.

[20] A. A. Knyazev, A. S. Krupin, and Y. G. Galyametdinov, "Composites based on polylactide doped with Amorphous Europium(III) complex as perspective thermosensitive luminescent materials," *Inorganics*, vol. 10, no. 12, 2022, Art. no. 232.

[21] Y. G. Galyametdinov, A. S. Krupin, and A. A. Knyazev, "Temperature-sensitive chameleon luminescent films based on PMMA doped with Europium(III) and Terbium(III) anisometric complexes," *Inorganics*, vol. 10, no. 7, 2022, Art. no. 94.

[22] G. E. Khalil et al., "Europium beta-diketonate temperature sensors: Effects of ligands, matrix, and concentration," *Rev. Sci. Instrum.*, vol. 75, no. 1, pp. 192–206, 2004.

[23] D. V. Lapaev, V. G. Nikiforov, V. S. Lobkov, A. A. Knyazev, and Y. G. Galyametdinov, "Reusable temperature-sensitive luminescent material based on vitrified film of Europium(III) -diketonate complex," *Opt. Mater.*, vol. 75, pp. 787–795, 2018.

[24] S. M. Borisov and O. S. Wolfbeis, "Temperature-sensitive Europium(III) probes and their use for simultaneous luminescent sensing of temperature and Oxygen," *Anal. Chem.*, vol. 78, no. 14, pp. 5094–101, 2006.

[25] H. Peng et al., "Luminescent Europium(III) nanoparticles for sensing and imaging of temperature in the physiological range," *Adv. Mater.*, vol. 22, no. 6, pp. 716–719, 2010.

[26] W. Becker, "Fluorescence lifetime imaging–techniques and applications," *J. Microsc.*, vol. 247, no. 2, pp. 119–136, 2012.

[27] R. Datta, T. M. Heaster, J. T. Sharick, A. A. Gillette, and M. C. Skala, "Fluorescence lifetime imaging microscopy: Fundamentals and advances in instrumentation, analysis, and applications," *J. Biomed. Opt.*, vol. 25, no. 7, 2020, Art. no. 071203.

[28] S. Medina-Rodríguez et al., "Improved multifrequency phase-modulation method that uses rectangular-wave signals to increase accuracy in luminescence spectroscopy," *Anal. Chem.*, vol. 86, no. 11, pp. 5245–5256, 2014.

[29] J. R. Lakowicz, *Principles of Fluorescence Spectroscopy*, 3rd ed. Berlin, Germany: Springer, 2006.

[30] D. Rife and R. Boorstyn, "Single tone parameter estimation from discrete-time observations," *IEEE Trans. Inf. Theory*, vol. 20, no. 5, pp. 591–598, Sep. 1974.

[31] C. Fitzgerald et al., "Fluorescence lifetime imaging of optically levitated aerosol: A technique to quantitatively map the viscosity of suspended aerosol particles," *Phys. Chem. Chem. Phys.*, vol. 18, no. 31, pp. 21710–21719, 2016.

[32] T. G. Euser, M. K. Garbos, J. S. Y. Chen, and P. St. J. Russell, "Precise balancing of viscous and radiation forces on a particle in liquid-filled photonic bandgap fiber," *Opt. Lett.*, vol. 34, no. 23, 2009, Art. no. 3674.

[33] R. K. P. Benninger et al., "Quantitative 3D mapping of fluidic temperatures within microchannel networks using fluorescence lifetime imaging," *Anal. Chem.*, vol. 78, no. 7, pp. 2272–2278, 2006.

[34] E. B. v. Munster and T. W. J. Gadella, "Suppression of photobleaching-induced artifacts in frequency-domain FLIM by permutation of the recording order," *Cytometry A: J. Int. Soc. Anal. Cytology*, vol. 58, no. 2, pp. 185–194, 2004.

[35] E. B. v. Munster, J. Goedhart, G. J. Kremers, E. M. M. Manders, and T. W. J. Gadella Jr., "Combination of a spinning disc confocal unit with frequency-domain fluorescence lifetime imaging microscopy," *Cytometry A: J. Int. Soc. Anal. Cytology*, vol. 71, no. 4, pp. 207–214, 2007.

[36] H. Szmacinski, V. Toshchakov, and J. R. Lakowicz, "Application of phasor plot and autofluorescence correction for study of heterogeneous cell population," *J. Biomed. Opt.*, vol. 19, no. 4, 2014, Art. no. 046017.

[37] J. R. Lakowicz, R. Jayaweera, N. Joshi, and I. Gryczynski, "Correction for contaminant fluorescence in frequency-domain fluorometry," *Anal. Biochem.*, vol. 160, no. 2, pp. 471–479, 1987.

Jasper Freitag received the M.Sc. degree in electrical, electronics, and communication engineering from Friedrich-Alexander-Universität (FAU), Erlangen-Nürnberg, Germany, in 2019. He is currently working toward the Ph.D. degree in electrical engineering with the Institute of Microwaves and Photonics, FAU. His research interests include microparticle traps, optical distance measurement techniques, and remote fiber optic sensors, with a specific focus on levitated particles trapped inside a hollow-core fiber for sensing.

Max Koeppel received the M.Sc. and Dr.-Ing. degree in electrical engineering from the Friedrich-Alexander-Universität (FAU), Erlangen-Nürnberg, Germany, in 2016 and 2023, respectively. His research interests include distributed fiber optic sensor systems, optical distance measurement techniques in the frequency domain, and related signal processing techniques.

Maria N. Romodina received the Ph.D. degree from Lomonosov Moscow State University, Moscow, Russia, in 2018. She is currently a Postdoctoral Fellow with the Max Planck Institute for the Physics of Light, Erlangen, Germany. Her research interests include applications of optical trapping and development of novel miniaturized devices for optical coherence tomography and Brillouin imaging.

Nicolas Y. Joly received the doctoral degree in physics from the University of Lille, Lille, France, in 2002. He then joined the group of Prof. Philip Russell with the University of Bath, Bath, U.K., as a Postdoctoral Fellow before returning to the University of Lille as a "Maître de conferences". Three years later, in 2009, he became Professor for experimental physics with the Friedrich-Alexander-Universität, Erlangen-Nürnberg, Germany. He has authored or coauthored more than 80 papers in international journals. His research interests include applications of photonic crystal fibres, from monitoring chemical reactions inside hollow-core fibre, to the generation of non-classical light using different types of microstructured optical fibre or the use of nonlinear effects in specially designed fibres. He is a Fellow of the Max Planck School of photonics, the Scientific coordinator of the International Max Planck School of Photonics, and a Senior Member of Optica Society.

Bernhard Schmauss (Member, IEEE) received the Dipl. Ing. and Dr.-Ing. degrees in electrical engineering from the Friedrich-Alexander-Universität (FAU), Erlangen-Nürnberg, Germany, in 1989 and 1995, respectively. In 1995, he joined Lucent Technologies, Nürnberg. He has been working on modelling and simulation of high-bit-rate optical communication systems. From 2001 to 2003, he was a Guest Professor of optical communication with FAU. From 2003 to 2005, he was a Professor with the University of Applied Sciences, Regensburg, Germany. Since 2005, he has been a Professor for optical microwaves and photonics with the Institute of Microwaves and Photonics, FAU. His research interests include fiber lasers, optical transmission systems, and fiber optical sensor systems. He is a Principal investigator of the Erlangen Graduate School in Advanced Optical Technologies and Fellow of the Max Planck School of Photonics.